JOURNAL OF CATALYSIS **145**, 1–9 (1994)

Selective Catalytic Reduction of NO with Methane on Gallium Catalysts

Yuejin Li and John N. Armor[1]

Air Products and Chemicals, Inc., 7201 Hamilton Boulevard, Allentown, 18195-1501

Received May 20, 1993; revised July 20, 1993

Gallium species supported on H–ZSM-5 and on H–mordenite are active catalysts for NO reduction with methane in the presence of excess O_2. Over Ga–H–ZSM-5, the NO reduction rate is first order in NO with a variable, fractional order in CH_4. The distinct feature of these gallium-based catalysts is their very high CH_4 selectivities for NO_x reduction. Ga–H–Y, on the other hand, is a poor catalyst for this reaction. The preparation method, ion exchange or wet impregnation, does not appear to be critical for the performance of a Ga/H–ZSM-5 catalyst. Gallium-exchanged and impregnated H–ZSM-5 have similar activities for the NO reduction. Comparable Brønsted acid sites were found on the H–ZSM-5 and the H–ZSM-5 supported gallium catalysts via temperature-programmed desorption measurements with ammonia and isopropylamine and by infrared measurements. On the other hand, the presence of H^+ in zeolite is important; Ga/Na–ZSM-5 was inactive for the NO reduction. It is apparent that a synergism exists between gallium species and H^+, and this serves to activate CH_4 as a reductant for NO in the presence of O_2. While Ga–H–ZSM-5 is more selective than Co–ZSM-5 for NO reduction, it is more sensitive to water, which makes it less attractive for commercial applications.

INTRODUCTION

Increasing public concerns about our environment and the ever stringent environmental regulations have stimulated extensive research in removal of NO_x from stationary and mobile sources. One of the currently practiced technologies is the selective catalytic reduction (SCR) of NO_x with ammonia. This technology is efficient in removing NO_x in an O_2-rich environment but has several shortcomings, such as ammonia slip (the breakthrough of the unreacted ammonia), equipment corrosion, and the transportation of ammonia through residential areas (1). Over the past few years, extensive work has proceeded to search for alternative reducing agents for NO_x, such as hydrocarbons. Propane, propene, ethylene, and more recently isobutane were found to selectively reduce NO_x in an O_2-rich atmosphere over a variety of catalysts (2–8). For NO reduction with propane, the most frequently studied catalyst is Cu–ZSM-5 (12), which is also an effective catalyst for the NO decomposition to its elements (9–11).

Recently, Li and Armor discovered CH_4 can be used to selectively reduce NO_x on certain metal-exchanged zeolites (13–16). Since natural gas, which contains >90% methane, is widely used as a fuel source for many combustion processes and electric utilities and is readily available in most parts of the world, its use as a reductant for NO_x would be desirable for industrial applications. Co-, Mn-, and Ni-exchanged zeolites such as ZSM-5 and mordenite are effective catalysts for the NO reduction with CH_4, but Cu–ZSM-5 is a poor catalyst because on Cu–ZSM-5, CH_4 preferably reacts with O_2 rather than with NO. Further, the presence of O_2 is essential for the reaction and the NO conversion is proportional to the CH_4 level in the feed. Neither Co^{2+}-exchanged Y nor CoO supported on alumina is active for this reaction. The active centers are believed to be the isolated metal ions which are activated by the zeolite lattice (15).

More recently, Ga-zeolites were reported, independently by Kikuchi and Yogo (17) and by Li and Armor (18), to be active for the NO reduction with methane. Here again the presence of O_2 is essential for the NO reduction. Previously, Ga-zeolites were reported active for NO reduction with propane having comparable activities to Cu–ZSM-5 (19). Ga/H–ZSM-5 is also reported to be more active than Cu–ZSM-5 for NO reduction by ethylene (20). In this paper, we report the NO reduction by CH_4 in the presence of O_2 over a variety of gallium-containing catalysts and compare them with Co–ZSM-5 as a catalyst.

EXPERIMENTAL

Materials

The exchange of gallium into ZSM-5 was attempted using a NH_4–ZSM-5 (a template-free synthesis with Si/

---

[1] To whom correspondence should be addressed.

0021-9517/94 $5.00

Al = 12) with an aqueous gallium nitrate solution (~0.01 *M*) at 80°C for 24 h. The initial pH of the Ga^{3+}/zeolite slurry was 2.9. After the exchange, the sample was washed, filtered, and dried at 110°C overnight. (It was further pretreated in situ with a flowing He at 500°C for 1 h before reaction.) The elemental analysis of this sample showed 35.9% Si, 2.97% Al, and 4.17% Ga by weight (Si/Al (atomic ratio) = 11.7, Ga/Al (atomic ratio) = 0.54), and the Na level was below the detection limit, i.e., <0.02% by weight. (Note, the Ga/Al ratios in the gallium-containing catalysts do not necessarily indicate the Ga^{3+} exchange levels because of precipitation of gallium species during the exchange process, *vide infra*.) This sample was designated as Ga–H–ZSM-5. Ga–H–mordenite was prepared via a two-step exchange process with a starting material, LZM-5 (a Na form of mordenite obtained from Linde). The Na–mordenite was first converted to the ammonium form by exchanging it with an NH_4NO_3 solution (12 cm^3 of 1 *M* NH_4 solution per g of zeolite) three times at room temperature. A near complete NH_4^+ exchange was obtained. The NH_4–mordenite was then exchanged with Ga^{3+} as described above. Ga–H–Y were prepared by exchanging $Ga(NO_3)_3$ with LZY-62 (an ammonium form of zeolite Y obtained from Linde). The gallium loadings were 5.3 wt% (Ga/Al atomic ratio = 0.40) and 8.9 wt% (Ga/Al atomic ratio = 0.37.) for Ga–H–mordenite and Ga–H–Y, respectively.

Gallium salts were also impregnated on H–ZSM-5, Na–ZSM-5, and γ-Al_2O_3 via the incipient wetness technique, and they are designated as Ga/H-ZSM-5, Ga/Na–ZSM-5, and Ga/Al_2O_3. H–ZSM-5 support was made by calcining the NH_4–ZSM-5 at 550°C for 4 h in air. The alumina support was a Kaiser/LaRoche Versal GH alumina with a surface area of 135 m^2/g, and the Na–ZSM-5 was prepared via a template-free synthesis with a Si/Al molar ratio of 12 (21). After impregnation, the resulting products were first dried at room temperature for 1 day in air, then at 100°C for 2 h. Finally they were calcined at 550°C in air for 2 h. All three of these impregnated gallium samples had an identical gallium loading, 3.2% by weight based on calculation.

Reaction Studies

The details of the catalytic activity measurements were described previously (12–14). Briefly, the activities were measured using a microcatalytic reactor operating in a steady-state plug flow mode. The reactor was a U-shaped glass tube with ¼″ o.d. at the inlet and ⅜″ o.d. at the outlet. The catalyst was pelletized, crushed, and then sieved to 60–80 mesh before use. Normally a 0.10 g sample was used for activity measurement. The reaction mixture was obtained by blending four channels of flow, i.e., NO/He, CH_4/He, O_2/He, and He, and each was controlled by an independent mass flow controller. All gases were obtained from Air Products and Chemicals, Inc., as certified standards and were used without further purification. The reaction mixture typically consisted of 1610 ppm NO, 1000 ppm CH_4, and 2.5% O_2 with He as the balancing gas, at a total flow rate of 100 cm^3/min. (The typical GHSV was 30,000 based on the apparent bulk density of the zeolite catalyst, ~0.5 g/cm^3.) A temperature programmer (Yokogawa, Model UP 40) with a J-type thermocouple in contact with the catalyst bed was used to control the temperature. [The catalyst was pretreated in situ in flowing He at 500°C for 1 h at a ramp rate of 5°C/min.] An on-line gas chromatograph with a TCD detector was used for the product analysis, and a molecular sieve 5A column was used to separate N_2, O_2, and CH_4. Formation of N_2 was used to calculate the NO conversion, and the CH_4 conversion was obtained by following the change in CH_4 peak area. The selectivity (α) is defined as the fraction of the reductant (CH_4) that is used up to reduce NO to N_2, i.e., the ratio of the consumption rate of CH_4 for the NO reduction (reaction [1]) to the total consumption rate of CH_4 (reaction [1] + reaction [2]), and α can be calculated based upon Eq. [3],

$$2NO + CH_4 + O_2 \rightarrow N_2 + CO_2 + 2H_2O \quad [1]$$

$$CH_4 + 2O_2 \rightarrow CO_2 + 2H_2O \quad [2]$$

$$\alpha = \frac{r_1}{r_t} = \frac{0.5 \times [NO]_0 \times C_{NO}}{[CH_4]_0 \times C_{CH_4}} \times 100\%, \quad [3]$$

where, $r_1 = 0.5 \times F_t \times [NO]_0 \times C_{NO}$, F_t is the total flow rate, $[NO]_0$ is the inlet concentration of NO, and C_{NO} is the conversion of NO; $r_t = F_t \times [CH_4]_0 \times C_{CH4}$. $[CH_4]_0$ is the inlet concentration of CH_4, and C_{CH4} is CH_4 conversion. The value, 0.5, is the stoichiometric ratio of NO to CH_4 (1 molecular of NO reacts with 0.5 molecule of CH_4). Consequently, (1 − α) is the fraction of CH_4 combusted O_2.

Characterization

Diffuse reflectance infrared spectra were collected using a Harrick HVC-DRP cell with a resolution of 0.5 cm^{-1}. A powder sample was packed in a sample holder and outgassed *in situ* by heating from 25 to 150°C at 5°C/min, holding the temperature at 150°C for 30 min, then ramping to 450°C at 5°C/min, and holding at 450°C for 1 h. The infrared spectra were collected at 25°C in vacuum after the pretreatment.

Temperature-programmed desorption (TPD) of ammonia was performed on Ga–H–ZSM-5, Ga/H–ZSM-5, H–ZSM-5, and Ga/Na–ZSM-5 using the micro-reactor system with an on-line mass spectrometer (UTI 100C). A 100-mg sample was used for the TPD measurement. The sample was first pretreated *in situ* in flowing He (100 cm^3/min) at 550°C for 1 h. It was then cooled to 100°C in He. Ammonia adsorption was carried out at 100°C by flowing an NH_3/He mixture (1% NH_3) through the sample for 20 min. The gas effluent was continuously monitored by the mass spectrometer, and an ammonia saturation was observed after the mixture had flowed for ~7 min, as indicated by the leveling off of MS signal. The sample was then flushed with He (150 cm^3/min.) at 100°C for 1 h. The TPD measurement was carried out in flowing He (150 cm^3/min.) from 100 to 550°C with a ramp rate of 8°C/min. The signals at AMU = 17 (NH_3) and 4 (He) were continuously collected, and the ammonia signals were normalized by those of He to cancel any sensitivity variations of the mass spectrometer during the measurement. The mass spectrometer was calibrated with NH_3/He mixtures from 1000 ppm to 1% NH_3, and quantitative desorption rates were calculated from TPD measurements.

Temperature-programmed desorption/decomposition (TPD) of isopropylamine [$(CH_3)_2CHNH_2$] was also carried out with the above five samples, providing an alternative approach to measure the Brønsted acid sites (22). The TPD measurements with isopropylamine were carried out with the same reactor system described above. A 35-mg sample underwent an *in situ* pretreatment (550°C in flowing He for 1 h) before the adsorption of isopropylamine. Isopropylamine (Aldrich product) was vaporized at 0°C via a saturator and carried to the reactor by a stream of He. The isopropylamine adsorption was carried out at 25°C (sample temperature) by flowing an isopropylamine/helium mixture through a sample. The sample was saturated with isopropylamine within one minute. The sample was then flushed with flowing He (150 cm^3/min) at 25°C for ~20 min to eliminate the gaseous and weakly adsorbed isopropylamine. TPD was measured at a ramp rate of 8°C/min and with a He flow rate of 150 cm^3/min. The signals at AMU = 4 (He), 17 (NH_3), 41 (a major fraction of C_3H_6), and 44 (a major fraction of isopropylamine) were continuously monitored by the mass spectrometer. TPD of NO was performed on Ga–H–ZSM-5, and the experimental procedures are similar to those described elsewhere (15).

The pore volumes of several gallium samples were measured on the McBain Bakr gravimetric adsorption balance. Before measurement, the zeolite samples were heated *in situ* to 400°C at 1°C/min and held at this temperature under a vacuum of less than 0.1 mTorr for 12 h. The oxygen adsorption was measured at liquid-nitrogen temperature (77 K) with an equilibrium O_2 pressure of 20 Torr. The weight gain due to the O_2 adsorption was recorded and normalized by the sample weight. The apparent O_2 density at 77 K within ZSM-5 was estimated as 0.92 g/cm^3, 80% of the density of liquid O_2, and used to calculate the pore volume (23). This is a useful approach to measure possible pore blockage with a zeolite.

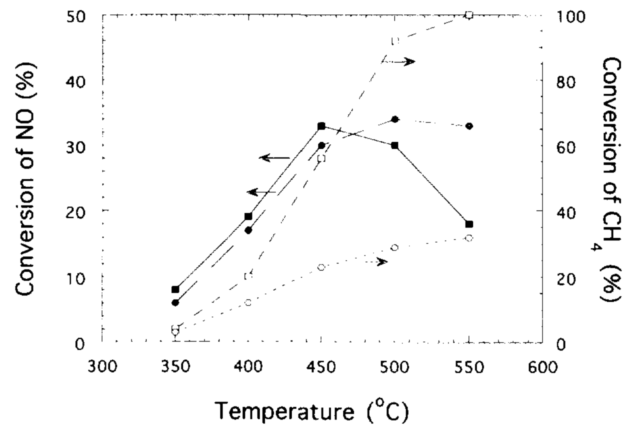

FIG. 1. Conversions of NO (solid symbols) and CH_4 (open symbols) as a function of reaction temperature over Ga–H–ZSM-5 (circles) and Co–ZSM-5 (squares). The reactions were run with a feed consisting of 1610 ppm NO, 1000 ppm CH_4, and 2.5% O_2 at a GHSV of 30,000.

RESULTS

Reaction Studies

The conversions of NO and CH_4 on Ga–H–ZSM-5 and Co–ZSM-5 are compared in Fig. 1 as a function of temperature. Ga–H–ZSM-5 has similar NO conversions compared to Co–ZSM-5 at temperatures between 350 to 450°C, and the conversion increases with temperature. Above 450°C, the NO conversion on Ga–H–ZSM-5 levels-off, while that on Co–ZSM-5 drops sharply. The difference in NO conversion on these two catalysts is most pronounced at 550°C, 33% on Ga–H–ZSM-5 and 18% on Co–ZSM-5. The difference in CH_4 conversion between these two catalysts is more dramatic. The CH_4 conversion on Co–ZSM-5 increases with temperature very steeply and reaches ~100% at $T > 500°C$. On Ga–H–ZSM-5, the CH_4 conversions are low and weakly dependent on temperature; the CH_4 conversion is only 32% at 550°C. Therefore the selectivity of CH_4 toward reacting with NO is much higher on Ga–H–ZSM-5 (100% at 450°C, which means CH_4 reacted with only NO without the needless combustion) than on Co–ZSM-5 (46% at 450°C), and this difference increases with temperature (82 and 22% at 550°C for Ga–H–ZSM-5 and Co–ZSM-5, respectively).

The dependence of NO and CH_4 conversions on the inlet CH_4 concentration over the Ga-H-ZSM-5 catalyst is shown in Fig. 2. Interestingly, the NO conversion increases very sharply with increasing CH_4 level at [CH_4] <400 ppm and gradually at 400 ppm < [CH_4] < 1200 ppm. Beyond [CH_4] = 1200 ppm, the NO conversion is constant with increasing [CH_4]. When plotting $\log(\text{rate})_{NO}$ vs

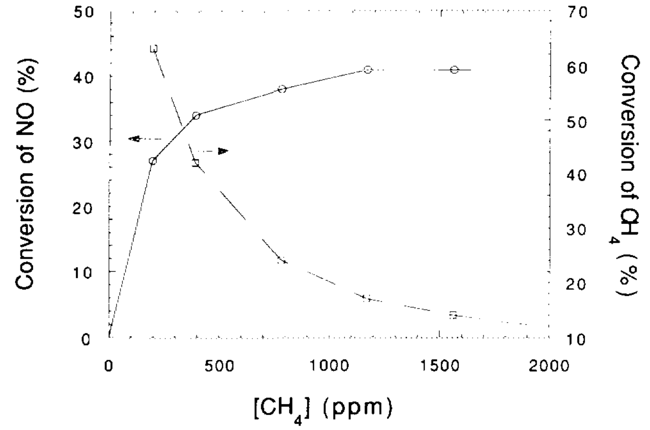

FIG. 2. Conversions of NO and CH_4 as a function of CH_4 inlet level on Ga–H–ZSM-5 at 500°C. The inlet [NO] = 800 ppm, $[O_2]$ = 2.5%, and GHSV = 30,000.

TABLE 1

NO Conversions[a] (%) for NO Reduction with CH_4 over Gallium Catalysts

Catalyst	Ga loading (wt%)	350°C	400°	450°C	500°C	550°C
Co-ZSM-5[a]	—	7	19	33	30	18
Ga-H-ZSM-5[b]	4.2	6	17	30	34	33
Ga/H-ZSM-5[c]	3.2	na	12	23	28	29
Ga/Na-ZSM-5[c]	3.2	na	<3	<3	<3	na
H-ZSM-5	—	—	4	6	10	na
Ga/Al_2O_3[c]	3.2	na	na	6	10	14
Al_2O_3	—	na	na	na	4	6
Ga-H-MOR[b]	5.3	8	16	22	27	31
Ga-H-Y[b]	8.9	na	3	3	4	4

Note. na: Activity not tested.

[a] The feed consists of 1610 ppm NO, 1000 pm CH_4, and 2.5% O_2, and the reactions were run with a GHSV of 30,000.

[b] Samples made by ion exchange.

[c] Samples made using the incipient wetness technique.

log($[CH_4]$), we do not obtain a straight line. At high CH_4 concentration, i.e., >1200 ppm, the empirical reaction rate order in CH_4 is zero and the reaction order increases with decreasing the $[CH_4]$. On the other hand, the CH_4 conversion decreases with increasing CH_4 concentration and is generally low, e.g., <30% for $[CH_4]$ >800 ppm. As a consequence, the selectivity of CH_4 for NO reduction in excess O_2 (not shown in Fig. 2) is relatively constant with varying $[CH_4]$, from 90% at 195 ppm CH_4 to 76% at 1950 ppm CH_4. The dependence of NO and CH_4 conversions on NO concentration is shown in Fig. 3. NO conversion is constant with inlet [NO], which is indicative of a first order reaction with respect to NO. There is a slight increase in CH_4 conversion with [NO], from 21% at 805 ppm NO to 29% at 1610 ppm NO. The calculated CH_4 selectivity increases with increasing NO concentration, from 68% at 805 ppm NO to 87% at 1610 ppm NO. In all cases, excess O_2 is present (2.5%). The very high CH_4 selectivity shown on Ga–H–ZSM-5 is not understood.

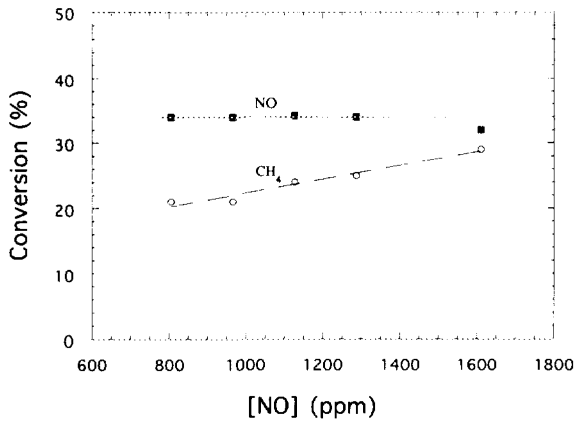

FIG. 3. Conversions of NO and CH_4 as a function of inlet NO level on Ga–H–ZSM-5 at 500°C. The inlet $[CH_4]$ = 1000 ppm, $[O_2]$ = 2.5%, and GHSV = 30,000.

To further investigate how the preparation method and support influence the NO reduction activity and to identify the active sites, a series of impregnated gallium samples, Ga/H-ZSM-5, Ga/Na-ZSM-5, and Ga/Al_2O_3 were tested for this reaction. Their activities are shown in Table 1. The NO conversions on Ga/H–ZSM-5 are slightly lower than those on Ga–H–ZSM-5. On the other hand, gallium impregnated on Na–ZSM-5, Ga/Na–ZSM-5, does not show appreciable activity for the NO reduction. H–ZSM-5 has low activity for this reaction. The NO conversions on Ga/Al_2O_3 are much lower than those of either Ga–H–ZSM-5 or Ga/H–ZSM-5 but similar to those of H–ZSM-5, with the highest conversion, 14%, at 550°C. Surprisingly, Al_2O_3 itself has some NO reduction activity, and its maximum conversion is 6% at 550°C. Ga–H–mordenite has similar NO reduction activities to Ga/H–ZSM-5. However, Ga–H–Y has a very low activity. Note that the CH_4 conversions on all the gallium catalysts, not shown in Table 1, are much lower than those on Co–ZSM-5; the highest CH_4 conversion is 32% obtained on Ga–H–ZSM-5 at 550°C. Here, we see the support has a very strong influence on the NO reduction activity of the gallium catalysts.

The effect of water vapor on the NO reduction activity was tested on Ga–H–ZSM-5. The NO conversion decreased from 40 to 13% upon addition of 2% H_2O at 500°C, and 16% was obtained at 550°C in the presence of H_2O. On a Co–ZSM-5 catalyst, however, the NO conversion decreases from 53 to 28% and from 40 to 35% at 450 and 500°C, respectively upon addition of 2% H_2O to the feed

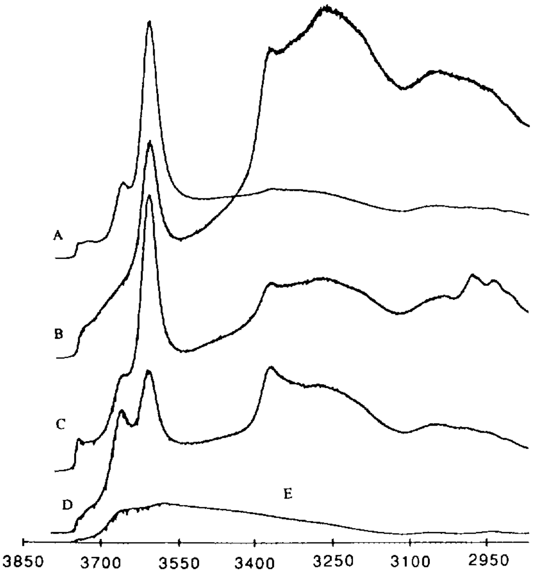

FIG. 4. Infrared spectra in OH region on H–ZSM-5 (A), fresh Ga–H–ZSM-5 (B), calcined Ga–H–ZSM-5 (C), Ga/H–ZSM-5 (D), and Ga/Na–ZSM-5 (E).

(GHSV = 30,000, 800 ppm NO, 1000 pm CH_4, and 2.5% O_2).

Infrared Analyses

Diffuse reflectance infrared spectra were collected on Ga–H–ZSM-5, Ga/H–ZSM-5, H–ZSM-5, and Ga/Na–ZSM-5 (see Fig. 4). After dehydration in vacuum at 450°C for 1 h, three bands at 3610, 3740, and 3660 cm^{-1} are identifiable in the OH region on H–ZSM-5 (A). The major band at 3610 cm^{-1} is attributed to the acidic, bridging OH. Two minor bands in the OH region at 3740 and 3660 cm^{-1} are assigned to the terminal SiOH and to the OH associated with extraframework Al, respectively. No OH band with appreciable intensity was observed on Ga/Na–ZSM-5 (E). On the uncalcined Ga–H–ZSM-5 (B), the band at 3660 cm^{-1} is not visible and the intensity of the band at 3610 cm^{-1} is noticeably lower than that of H–ZSM-5 (A). Further, the NH stretching bands of NH_4^+ species were observed at ~3373 and ~1460 cm^{-1} (the latter is not shown in the figure), which suggests that the NH_4^+ in the zeolite was not completely decomposed to H^+ during the *in situ* dehydration. The broad band at <3300 cm^{-1} is due to hydrogen-bonding. Upon calcination of this sample at 600°C (C), the intensity of the band at 3610 cm^{-1} increased significantly (to the level comparable to that on H–ZSM-5) while the NH stretching bands decreased, and the band at ~1460 cm^{-1} disappeared. The band at 3660 cm^{-1} also became visible. On Ga/H–ZSM-5 (D), the impregnated sample, the intensity of the band at 3610 cm^{-1} seems substantially lower than either H–ZSM-5 or the calcined Ga–H–ZSM-5. On the other hand, the band at 3660 cm^{-1} seems to have increased.

TPD of Ammonia

The ammonia TPD profiles on different gallium samples are shown in Fig. 5. Two weakly bound ammonia desorption peaks appear at ~170 and 210°C. The high-temperature ammonia desorption peak, ~375°C, is due to the Brønsted acidity of zeolite. This peak is completely missing on Ga/Na–ZSM-5, suggesting the absence of Brønsted acidity for this sample. The amounts of ammonia desorbed from the high-temperature peak are integrated and shown in Table 2. The amount of NH_3 desorbed at high temperature over the fresh Ga–H–ZSM-5 is about 1 NH_3 per 1 Al, which is even higher than that of H–ZSM-5, 0.77. However, after calcination of Ga–H–ZSM-5 at 550°C for 4 h (the same thermal treatment performed to prepare H–ZSM-5) the NH_3/Al ratio, 0.77, was obtained. Therefore, there is about the same amount of H^+ in Ga–H–ZSM-5 as in H–ZSM-5. This suggests that most of NH_4^+ in NH_4–ZSM-5 was not exchanged out by Ga^{3+} cations. The NH_3/Al ratio for Ga/H–ZSM-5 is slightly lower than that of H–ZSM-5, which may be due to the extra calcination time. The TPD experiments were repeated using a thermogravimetric technique with a 20-mg sample, and similar results were obtained.

TPD of Isopropylamine

A TPD measurement with isopropylamine on Ga–H–ZSM-5 is shown in Fig. 6. Isopropylamine desorption was observed at 80, 160, and 340°C, and at ~340°C significant amount of isopropylamine decomposition products, propene and ammonia, were observed with the

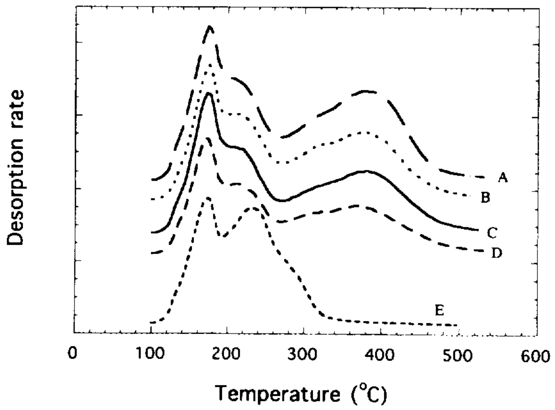

FIG. 5. TPD of ammonia profiles of fresh Ga–H–ZSM-5 (A), calcined Ga–H–ZSM-5 (B), H–ZSM-5 (C), Ga/H–ZSM-5 (D), and Ga/Na–ZSM-5 (E).

TABLE 2

Quantification of Ammonia and Isopropylamine TPD Measurements

Sample	Preparation method	Calcination time[a] (h)	TPD of ammonia: Ammonia desorbed[b] (mmol/g)	TPD of ammonia: NH_3/Al^c	TPD of isopropylamine: Propene formation (mmol/g)	TPD of isopropylamine: C_3H_6/Al^c
H–ZSM-5	Cal. NH_4–ZSM-5	4	0.85	0.77	0.95	0.87
Ga–H–ZSM-5	Ion exchange	0	1.05	0.95	1.16	1.05
		4	0.85	0.77	0.95	0.87
Ga/H–ZSM-5	Impregnation	6	0.70	0.64	0.80	0.73
Ga/Na-ZSM-5	Impregnation	2	0.0	0.0	0.0	0.0

[a] The samples were calcined in air at 550°C for various periods of time. The calcination times shown in this table do not include the *in situ* pretreatment with He prior to the TPD measurement.

[b] The NH_3 desorptions were based on the integrations of the high-temperature desorption peaks (see Fig. 5).

[c] Bulk aluminum content is used, which is 1.1 mmol/g.

ammonia desorption shifting to a slightly higher temperature. According to Parrillo *et al.* (24), his high temperature decomposition of isopropylamine is catalyzed by the Brønsted acid sites. The amount of propene formed is 1.16 mmol/g (integrated based on the desorption rate vs time). The TPD profiles on H–ZSM-5, Ga–H–ZSM-5 (precalcined), and Ga/H–ZSM-5 are very similar with only slight variations in the amount of propene formation. On Ga/Na–ZSM-5, the high-temperature decomposition feature was not observed, and the amount of isopropylamine reversibly desorbed is comparable to those of other samples. The propene formation on all samples are quantified and given in Table 2. These results are consistent with those measured with ammonia.

Pore Volume Measurements

To test whether gallium is inside or outside the zeolite pores, the effective pore volumes of Ga–H–ZSM-5, Ga/H–ZSM-5, and H–ZSM-5 were measured. The results are shown in Table 3. Based on the gross weight of the samples, the pore volumes of gallium containing samples do indicate some decrease, ~7%, compared to H–ZSM-5. However, the introduction of gallium contributes to the sample weight but little to pore volume. The corrected pore volumes based on the weight of zeolite are similar. [The differences are within ±2%.] Note, if all the gallium in Ga–H–ZSM-5 is within the zeolite pores we would expect a corrected pore volume reduction of ~0.01 cm^3/g or ~5.5% (calculated based on the Ga_2O_3 density of 5.88 g/cm^3). This suggests that not all the gallium species are inside the zeolite pores.

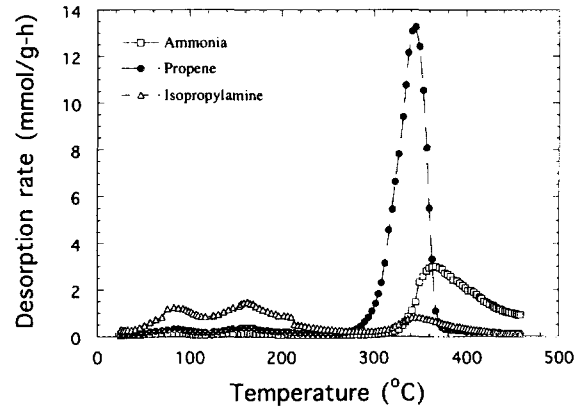

FIG. 6. TPD of isopropylamine on Ga–H–ZSM-5.

TPD of NO

We carried out a NO adsorption/TPD experiment on Ga–H–ZSM-5. We found no detectable NO uptake at room temperature, and consequently no NO desorbed during the TPD experiment. Alternatively, when a mixture of NO/He (1600 ppm NO) was passed through the catalyst, while ramping the temperature from 25 to 500°C, no detectable NO consumption was observed at any tem-

TABLE 3

Pore Volumes of the Zeolite Samples

Sample	Pore volume[a] (cm^3/g)	Corrected pore volume[b] (cm^3/g)
H–ZSM-5	0.182	0.182
Ga–H–ZSM-5	0.169	0.179
Ga/H–ZSM-5	0.170	0.178

[a] Based on gross weight of a sample, which may include the weight of Ga_2O_3.

[b] Based on the zeolite weight only.

perature. This suggests that the interaction between NO and Ga–H–ZSM-5 is weak.

DISCUSSION

For the NO reduction on a Co-zeolite catalyst, the isolated cobalt cations are the active sites whereas supported cobalt oxide particles are inactive (14–16). It is, therefore, reasonable to expect that gallium is also exchanged into the zeolite sites as cations. If most of the gallium were exchanged into the zeolite sites, we would expect NH_4^+ being exchanged out of the zeolite, and after calcination, the sample should display decreased Brønsted acidity. However, our IR data indicate that a significant amount of NH_4^+ still remains in the zeolite. The OH band intensities of the gallium exchanged ZSM-5 and H–ZSM-5 are similar after calcination of Ga–NH_4–ZSM-5 at 600°C. More quantitative analysis of the Brønsted acidity is provided by the TPD experiments with both ammonia and isopropylamine. After identical thermal treatment of samples, we obtained the same amount of Brønsted acidity on H–ZSM-5 and Ga–H–ZSM-5 with an identical peak-shape, indicating that most of the ammonium ions were not exchanged out in the gallium solution. Based on these results, we believe that the gallium in Ga–H–ZSM-5 is mainly precipitated on, rather than exchanged into, ZSM-5. This is support by the pore volume data supplied in Table 3. [Note, this does not exclude the possibility that small amount Ga^{3+} may be exchanged into NH_4–ZSM-5 either during its preparation or during the high temperature, *in situ* treatment.]

Similar observations were made by others on the Ga–H–ZSM-5 system active for aromatization of light alkanes. Tan *et al.* (25) found the Brønsted acidity of Ga–H–ZSM-5 (exchanged), as measured by infrared spectroscopy of pyridine adsorption, is essentially the same compared to that of the starting zeolite, H–ZSM-5. Using hexane cracking as a probe for Brønsted acidity, Kitagawa *et al.* (26), obtained essentially the same hexane conversion on both H–ZSM-5 and the Ga–H–ZSM-5 (exchanged). They concluded that the acidic property of H–ZSM-5 is not altered by the gallium exchange, which is also consistent with their temperature-programmed desorption measurements with ammonia. Yakerson *et al.* (27) made Ga–H–ZSM-5 by ion exchange followed by impregnation with the mother solution. The resulting sample was analyzed by analytical microscopy and most of the gallium was found as a Ga_2O_3 phase and located on the outer surface of zeolite grains. This conclusion is supported by others (28, 29) and explains the similarity in NO reduction activity between Ga–H–ZSM-5 ("ion exchanged") and Ga/H–ZSM-5 (impregnated) catalysts.

Precipitation of Ga species during the ion exchange process may occur and be due to the hydrated gallium cation being too large to enter the internal pores of the ZSM-5 zeolite, as suggested in the literature (28). On the other hand, the solubility constant for $Ga(OH)_{3(s)}$ ($Ga(OH)_{3(s)} = Ga^{3+} + 3OH^-$) is very small, K = ca. 5×10^{-37} (30). Based only on this equilibrium and a solution pH of ~3, we would expect precipitation of $Ga(OH)_3$ occur at $[Ga^{3+}] \geq 5 \times 10^{-4}$ M. The fact that we did not observe precipitation with a 0.01 M $Ga(NO_3)_3$ solution (in the absence of zeolite) suggests other equilibria also are taking place, such as $GaOH^{2+} = Ga^{3+} + OH^-$, $K = 4 \times 10^{-12}$; and $Ga(OH)_2^+ = Ga(OH)^{2+} + OH^-$, $K = 1.6 \times 10^{-11}$. It is difficult to evaluate the concentrations of all gallium species in a solution in the presence of the zeolite. However, it is possible that the local concentrations of Ga^{3+} inside zeolite cages are high enough to cause $Ga(OH)_3$ precipitation. We attempted to identify a gallium oxide phase in a calcined Ga–H–ZSM-5 by XRD but were not successful due to interference with zeolite peaks.

It is apparent that the Brønsted acidity in gallium catalysts is very important; Ga/H–ZSM-5 is active for the NO reduction but Ga/Na–ZSM-5 is not. The presence of Brønsted acidity or gallium oxide alone is much less active than the combination of both (see Table 1). Yet, the exchange or impregnation by gallium ions does not significantly alter the Brønsted acidity (Table 2). There must be some synergistic effect between the gallium species and the H^+ in the zeolite. Possibly, the role of gallium is to enhance the activation of CH_4 with the NO reduction occurring on H^+ sites, or vice versa. This may be analogous to that suggested (31, 32) in propane aromatization reaction on Ga–H–ZSM-5, where C_3H_8 is dehydrogenated on the gallium phase to form $C_3H_7^+$ carbenium ion, which subsequently reacts with the Brønsted acid sites of the zeolite. Buckles *et al.* (33) further proposed that C–H bond polarization occurs in C_3H_8 on Ga_2O_3 as an initial step and that the C–H bond cleavage is facilitated by the interaction of the polarized C–H bond with the Brønsted acid sites of zeolite.

The type of zeolite is shown to be important; Ga–H–ZSM-5 and Ga–H–mordenite are active for the NO reduction but Ga–H–Y is not. A similar observation was made when propane was used as a reducing agent for NO (19). It seems that there is an intimate, cooperative interaction between H-zeolite and gallium, where the zeolite exerts its influence (via either its shape selectivity, acidity or the crystal field) on the gallium. This type of interaction is more likely occurring on those sites where Ga^{3+} and H^+ are within proximity in zeolite pores. A small amount of Ga^{3+} might also be exchanged into the H-zeolites driven by the $Ga_2O_3 + H^+$ reaction at high temperatures, whereas the ion exchange is impossible in Na–ZSM-5. In light of this analysis, the small amount of gallium within zeolite pores are catalytically more important. The effect of zeolite is also evident in other catalytic systems. Co-exchanged ZSM-5 and mordenite are good catalysts for the NO reduction by CH_4, whereas Co–Y is a poor catalyst (14). Similarly, both Cu- and Co-exchanged ZSM-5 and mordenite are excellent catalysts for the N_2O decomposition, but Cu and Co supported on zeolite Y are less active (34). Perhaps these phenomena are related. The lattice oxygen may be involved in the reactions. Recent work indicates that zeolite lattice oxygen may be involved extensively in the NO decomposition reaction on Cu–ZSM-5 (35), and oxygen mobility in zeolite may be a key factor for reactions that involve oxygen. For NO reduction with CH_4, the presence of O_2 is essential, in fact NO_2 can be effectively reduced in the absence of O_2. It is conceivable that the zeolites having high lattice oxygen mobility will provide a more readily available source of activated oxygen, which is reflected in the high selectivities for reactions such as $NO + CH_4 + O_2$ vs CH_4 combustion. Several interesting questions related to the role of gallium remain unanswered. Our work with $NO + CH_4 + O_2$ further demonstrates the importance of the presence of gallium on H–ZSM-5 as previously described for aromatization reactions.

Two different mechanisms appear to be operating for the NO reduction over Co–ZSM-5 vs Ga–ZSM-5, and this difference is probably related to their very different active centers. It is known that on Co–ZSM-5, NO adsorbed at room temperature with $NO/Co > 1$, and all the NO desorbed at $T < 400°C$ in a He flow as determined by TPD (15). The NO adsorption is essential to its reduction by CH_4. On Ga–H–ZSM-5, however, there is no appreciable NO adsorption at room temperature or at elevated temperatures. Therefore the interaction between NO and Ga is very weak. Unlike Co–ZSM-5, on which NO conversion decreases with increasing NO partial pressure in a dry feed, the NO conversion on Ga–H–ZSM-5 is constant with NO partial pressure, which means that NO reduction on Ga–H–ZSM-5 is first order in NO. The peculiar dependence of NO conversion on CH_4 partial pressure suggests that gallium catalysts are capable of effectively activating CH_4, which is the key for the high selectivity of this reaction for gallium catalysts. However, on a gallium catalyst, simply increasing the CH_4 concentration in the feed can only enhance the NO conversion to a certain point.

From practical point of view, the tolerance of water vapor by a de-NO_x catalyst is very important because flue gas steams contain high levels of water vapor. Looking at Table 1, one can conclude that Ga–H–ZSM-5 is an active catalyst for NO reduction by CH_4 in the presence of O_2. However, the gallium based catalysts suffer a much greater loss in activity upon exposure to 2% water vapor, as compared to Co–ZSM-5. This may be related in some way to the different mechanistic pathways for Ga–H–ZSM-5 vs Co–ZSM-5 or to different degrees of hydrolysis of the two elements. For the moment, the cobalt based zeolite catalysts are more effective in the presence of water vapor than those incorporating gallium.

CONCLUSIONS

Gallium supported on H–ZSM-5 is a very selective catalyst for the reduction of NO with CH_4 in the presence of excess O_2. The NO reduction rate is first order in NO partial pressure with varied, fractional orders in CH_4 partial pressure. The preparation method for Ga/H–ZSM-5 is not important for achieving NO reduction activity. Gallium in Ga–H–ZSM-5 was found mainly as precipitated gallium, as evidenced by the presence of comparable amounts of H^+ in the Ga–H–ZSM-5 catalysts compared to that of pure H–ZSM-5. The Na–ZSM-5 supported gallium is not active for the NO reduction by CH_4, and the presence of Brønsted acidity appears essential. There appears to be some synergism between gallium species and H^+ in ZSM-5 with regard to NO reduction by CH_4. Further, the type of zeolite is important for the NO reduction activity. Ga–H–ZSM-5 and Ga–H–mordenite are active catalysts, but Ga–H–Y is not.

Ga–H–ZSM-5 differs from Co–ZSM-5 in several ways; methane is more selective for NO reduction on the gallium catalyst, and the interaction between NO and Ga is weaker. Therefore, the mechanisms for the NO reduction appear to be very different. Unfortunately, Ga–H–ZSM-5 is more sensitive to water vapor than is Co–ZSM-5.

ACKNOWLEDGMENTS

Thanks are due to Paula Battavio for the activity measurements and to Terry Slager for the infrared measurements. Helpful discussions with Keith Hall are greatly acknowledged. We thank Air Products and Chemicals, Inc., for permission to publish this work.

REFERENCES

1. Bosch, H., and Janssen, F., *Catal. Today* **2,** 369 (1988).
2. Hamada, H., Kintaichi, Y., Sasaki, M., Ito, T., and Tabata, M., *Appl. Catal.* **64,** L1 (1990).
3. Kintaichi, Y., Hamada, H., Tabata, M., Sasaki, M., and Ito, T., *Catal. Lett.* **6,** 39 (1990).
4. Hamada, H., Kintaichi, Y., Sasaki, M., Ito, T., and Tabata, M., *Appl. Catal.* **70,** L15 (1991).
5. Misono, M., and Kondo, K., *Chem. Lett.* 1001 (1991).
6. Sato, S., Yu-U., Y., Yahiro, H., Mizuno, N., and Iwamoto, M., *Appl. Catal.* **70,** L1 (1991).
7. Sato, S., Hirabay, H., Yahiro, H., Mizuno, N., and Iwamoto, M., *Catal. Lett.* **12,** 193 (1992).
8. Petunchi, J. O., Sill, G., and Hall, W. K., *Appl. Catal.* **B2,** 303 (1993).
9. Iwamoto, M., *in* "Future Opportunities in Catalytic and Separation Technologies" (M. Misono, Y. Moro-oka, and S. Kimura, Eds.), p. 121. Elsevier, Amsterdam, 1990.
10. Li, Y., and Hall, W. K., *J. Catal.* **129,** 202 (1991).

11. Li, Y., and Armor, J. N., *Appl. Catal.* **76,** L1 (1991).
12. Truex, T. J., Searles, R. A., and Sun, D. C., *Platinum Met. Rev.* **36**(1), 2 (1992).
13. Li, Y., and Armor, J. N., U.S. Patent, 5149512, (1992).
14. Li, Y., and Armor, J. N., *Appl. Catal. B* **1,** L31 (1992).
15. Li, Y., and Armor, J. N., *Appl. Catal. B* **2,** 239 (1993).
16. Li, Y., Battavio, P. J., and Armor, J. N., *J. Catal.* **142,** 561 (1993).
17. Kikuchi, E., and Yogo, K., Presented at Inter. Forum on Envir. Catal.-'93, Tokyo, Japan, Feb. 4–5, 1993.
18. Li, Y., and Armor, J. N., U.S. Patent (allowed).
19. Yogo, K., Tanaka, S., Ihara, M., Hishiki, T., and Kikuchi, E., *Chem. Lett.*, 1025 (1992).
20. Yogo, K., Ihara, M., Terasaki, I., and Kikuchi, E., *Catal. Lett.* **17,** 303 (1993).
21. Shirahar, V. P., and Clearfield, A., *Zeolite* **9,** 363 (1989).
22. Kofke, T. J. G., Gorte, R. J., and Kokotailo, G. T., *J. Catal.* **115,** 265 (1989).
23. Carrot, P. J. W., Roberts, R. A., and Sing, K. S. W., *Chem. Ind.*, 855 (1987).
24. Parrillo, D. J., Adamo, A. T., Kokotailo, G. T., and Gorte, R. J., *Appl. Catal.* **67,** 107 (1990).
25. Tan, C., Cheng, C., Zhou, L., and Peng, S., *in* "Proceedings, 9th International Congress on Catalysis, Calgary, 1988," (M. J. Phillips and M. Ternan, Eds.), p. 445. Chem. Institute of Canada, Ottawa, 1988.
26. Kitagawa, H., Senoda, Y., and Ono, Y., *J. Catal.* **101,** 12 (1986).
27. Yakerson, V. I., Vasina, T. V., Lafer, L. I., Stynyk, V. P., Dykh, Z. H. L., Mokhov, A. V., Bragin, O. V., and Minachev, K. H. M., *Catal. Lett.* **3,** 339 (1989).
28. Kazansky, V. B., Kustov, L. M., and Yu Khodakov, A., *Stud. Surf. Sci. Catal.* **49,** 1173 (1989).
29. Joly, J. F., Ajot, H., Merlen, E., Raatz, F., and Alario, F., *Appl. Catal. A* **19,** 249 (1991).
30. Latimer, W. M., *in* "Oxidation Potentials," 2nd Printing, p. 158 ff. Prentice-Hall, Englewood Cliffs, NJ, 1953.
31. Merriaudeau, P., and Naccache, C., *J. Mol. Catal.* **59,** L31 (1990).
32. Bayense, C. R., van der Pol, A. J. H. P., and van Hooff, J. H. P., *Appl. Catal.* **72,** 81 (1991).
33. Buckles, G., Huchings, G. J., and Williams, G. D., *Catal. Lett.* **11,** 89 (1991).
34. Li, Y. and Armor, J. N., *Appl. Catal. B* **1,** L21 (1992).
35. Valyon, J., and Hall, W. K., *J. Catal.*, **143,** 520 (1993).